SPINE Volume 28, Number 5, pp 455–462
©2003, Lippincott Williams & Wilkins, Inc.

Prediction of Osteoporotic Spinal Deformity

Tony S. Keller, PhD,* Deed E. Harrison, DC,† Christopher J. Colloca, DC,‡
Donald D. Harrison, DC, PhD,§ and Tadeusz J. Janik, PhD‖

Study Design. A biomechanical model was developed from full-spine lateral radiographs to predict osteoporotic spinal deformity in elderly subjects.

Objective. To investigate the biomechanics of age-related spinal deformity and concomitant height loss associated with vertebral osteoporosis.

Summary of Background Data. Vertebral bone loss and disc degeneration associated with aging causes bone and disc structures to weaken and deform as a result of gravity and postural stresses.

Methods. An anatomically accurate sagittal-plane, upright-posture biomechanical model of the anterior spinal column (C2–S1) was created by digitizing lateral full-spine radiographs of 20 human subjects with a mean height of 176.8 cm and a mean body weight of 76.6 kg. Body weight loads were applied to the model, after which intervertebral disc and vertebral body forces and deformation were computed and the new spine geometry was calculated. The strength and stiffness of the vertebral bodies were reduced according to an osteopenic aging model and modulus reduction algorithm, respectively.

Results. The most osteopenic model (L3 F_{ult} = 750 N) produced gross deformities of the spine, including anterior wedge-like fracture deformities at T7 and T8. In this model, increases in thoracic kyphosis and decreases in vertebral body height resulted in a 25.2% decrease in spinal height (C2-S1), an 8.6% decrease in total body height, and a 15.1-cm anterior translation of the C2 spine segment centroid. The resulting deformity qualitatively resembled deformities observed in elderly individuals with osteoporotic compression fractures.

Conclusions. These predictions suggest that postural forces are responsible for initiation of osteoporotic spinal deformity in elderly subjects. Vertebral deformities are exacerbated by anterior translation of the upper spinal column, which increases compressive loads in the thoracolumbar region of the spine. [Key words: biomechanicalmodeling, deformity, fracture, kyphosis, osteoporosis, posture, spine] **Spine 2003;28:455–462**

From the *Departments of Mechanical Engineering and Orthopaedics and Rehabilitation, University of Vermont, Burlington, Vermont, the †Ruby Mountain Chiropractic Center, Elko, Nevada, the ‡Postgraduate and Continuing Education Department, New York Chiropractic College, Seneca Falls, New York, and State of the Art Chiropractic Center, P.C., Phoenix, Arizona, the §Biomechanics Laboratory, Université du Québec a Trois-Rivières, Canada, and ‖CompMath R/C, Huntsville, Alabama.
Presented in part at the 2002 International Society for the Study of the Lumbar Spine, May 14–18, Cleveland, Ohio, and received the Sofamor Danek Group Oral Poster Presentation Award.
Acknowledgment date: June 4, 2002. First revision date: July 26, 2002. Acceptance date: July 30, 2002.
Device status/drug statement: The manuscript submitted does not contain information about medical device(s)/drug(s).
Conflict of interest: Federal, Institutional, and Foundation funds were received in support of this work. No benefits in any form have been or will be received from a commercial party related directly or indirectly to the subject of this manuscript.
Address reprint requests to Tony S. Keller, PhD, Department of Mechanical Engineering, University of Vermont, 119C Votey Building, Burlington, VT, 05405-0156. E-mail: keller@emba.uvm.edu.

In the United States, 10 million individuals have a diagnosis of osteoporosis. Another 18 million have low bone mass, which places them at increased risk for osteoporosis and fracture. It is estimated that 500,000 white women in the United States experience vertebral deformities for the first time each year, and that more than 7 million white women 50 years of age and older may be affected at any given time.[29] The cost for treatment of osteoporotic fracture is estimated to reach $15 billion annually.[31] Vertebral compression and compression–flexion fractures, particularly anterior wedge fractures in the middle and lower thoracic region, produce spinal deformities characterized by increased thoracic kyphosis and associated with significant performance impairments in physical, functional, and psychosocial domains.[12,28]

The normal spine is characterized by a thoracic kyphosis of approximately 40° when measured between T2 and T10.[4,9,19] A single anterior wedge fracture can increase thoracic kyphosis by 10° or more, and thoracic curves exceeding 70° are common in elderly subjects with multilevel compression fractures (Figure 1). In a study of 98 elderly, postmenopausal women, Cortet *et al*[5] reported a mean thoracic kyphosis increase of 11° in osteoporotic women with radiographic evidence of fracture, as compared with women who had no radiographic evidence of fracture (mean kyphosis, 52°). Moreover, the severity of thoracic kyphosis has been shown to increase with decreasing bone mineral density (BMD)[9] and anterior translation of the thorax.[17] In advanced osteoporosis, compression fractures of the thoracic vertebrae, particularly T6 and T7, result in a loss of vertebral height, wedging of several thoracic vertebrae, and formation of a kyphotic deformity or "Dowager's Hump."[37] This deformity often is associated with severe pain and loss of mobility.[12,28]

Given the fragility of osteoporotic vertebrae,[13] trauma is not necessarily a factor in the production of fractures in the thoracic spine. As postulated by Schmorl and Junghanns,[37] "the cause is usually to be found in the stresses of everyday life."(pg. 65) Thus, in the presence of osteoporosis, postural stresses alone are sufficient to produce collapse at the anterior margins of the thoracic vertebral bodies and the resulting wedge deformity.

Keller and Nathan[23] developed an upright-posture, sagittal-plane model of the C2–S1 spine, which they used to estimate disc forces and stresses as well as the concomitant diurnal changes in disc height and stature associated with upright posture loading. Vertebral body (VB) and intervertebral disc (IVD) geometries were modeled as quadrilaterals. Static equilibrium forces and moments were computed about each IVD centroid for forces asso-

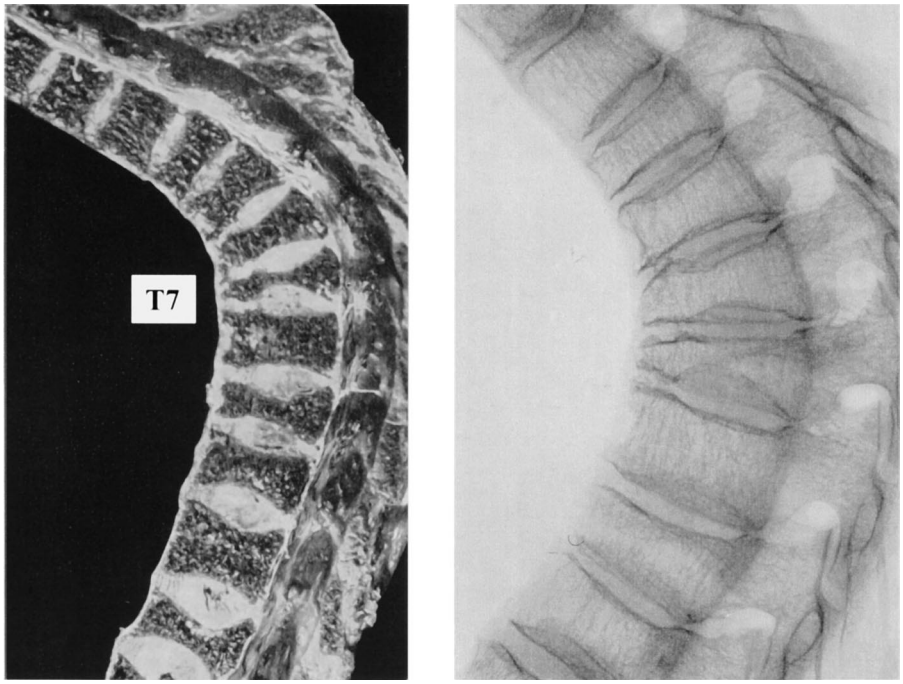

Figure 1. Left: Photomicrograph of the thoracic spine of a 63-year-old woman with an osteoporotic thoracic kyphosis (≈80°) produced by vertebral wedge fractures (T6, T7). Right: Radiograph of same specimen. (adapted from Schmorl and Junghanns[37])

ciated with the body weight (LOG) and activity of the antigravity muscles (erector spinae muscles). This model predicted that IVD compressive forces and stresses associated with upright posture weightbearing were greatest in the middle and lower thoracic region of the spine.

The objective of the current study was to adapt the upright posture model of Keller and Nathan[23] to predict kyphotic spine deformities associated with osteoporosis. The authors hypothesized that in subjects with advanced osteoporosis, postural forces are sufficient to initiate thoracic spine kyphotic deformities, which are subsequently exacerbated by anterior translation of the head and upper torso.

■ Methods

An anatomically accurate sagittal-plane biomechanical model of the anterior spinal column (C2–S1) was created using radiographic data obtained from lateral full-spine views of neutral-posture, upright-standing human subjects (n = 20; mean height, 176.8 cm; mean body weight, 76.6 kg). Anterosuperior, posterosuperior, anteroinferior, and posteroinferior corners of each vertebral body were marked using a sonic digitizer (GP-9; GTCO CalComp, Columbia, MD). The resolution of the sonic digitizer was 0.125 mm, and the average accuracy of multiple attempts at digitizing the chosen origin point on the radiographs was 0.5 mm. This resolution and accuracy were sufficient to capture the gross anatomic features of the VB and IVD geometry. The resulting VB coordinate geometry data of the 20 subjects were averaged and stored in a text file for processing.

Vertebral Loading Model. Figure 2 illustrates the C2–S1 quadrilateral-element, sagittal-plane, upright-posture biomechanical model of the spine,[23] which has been adapted to predict anterior and posterior VB deformations and to account for age-related bone degeneration (bone loss, strength reduction) and load-dependent VB stiffness reduction.[25] Postural forces were based on the body weight load above each vertebral segment, with the line of gravity (LOG) initially positioned 10 mm anteriorly to the centroid of the L4 vertebral body (Figure 2). The locations of the LOG, the body weight load above each segment (W), the values for the posterior muscle moment arms (l_E), and the disc cross-sectional areas for the C2–S1 segments were based on previously published data.[23,33] Only the anterior column of the spine was considered, and ligamentous structures were not explicitly modeled.

Compressive loads (C) and shear loads (S) at each VB and IVD centroid and the resultant extensor muscle load (E) were determined according to the static equilibrium analysis of Nathan and Keller[23] (Figure 2).

Vertebral Deformity Model. Anterior VB deformation (d_A) and posterior VB deformation (d_P) were computed using the following equations obtained from the static equilibrium of forces and moments about each quadrilateral VB element centroid:

$$d_P = 9.81W(l_W/l_E + \cos\alpha)/\{k[(h_A/h_P)(1 + l_A/l_E) - l_P/l_E + 1]\} \quad (1)$$

$$d_A = d_P(h_A/h_P)P \quad (2)$$

where W is the body weight above each segment (kg), l_W is the body weight moment arm (mm), l_E is the posterior muscle moment arm (mm), α is the quadrilateral anteroposterior bisector angle (radians) with respect to horizontal, h_A is the anterior VB height (mm), h_P is the posterior VB height (mm), l_A is the anterior VB load moment arm (mm), l_P is the posterior VB load moment arm (mm), k is the VB stiffness (N/mm), and p is an empirical constant. Equation 1 was required to solve the system of static equilibrium equations for the loads acting on the anterior and posterior aspects of the VB quadrilateral segments (A and P, respectively in Figure 2). A parametric analysis of the effects of scaling parameter p on the thoracic angle was performed, and a p value of 2 was found to produce the most realistic deformities (Figure 3A). The VB stiffness (k) of each

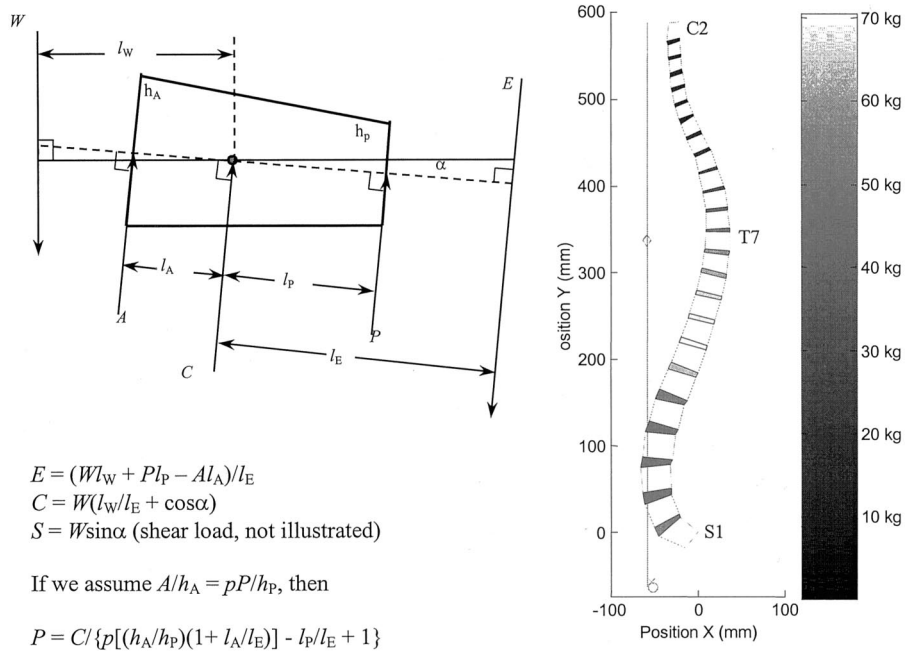

Figure 2. Quadrilateral-element intervertebral disc (IVD) and vertebral body (VB) deformity model of the C2–S1 spine. *W,* body force vector; *E,* extensor muscle force; *C,* compressive force at centroid; *S,* shear force at centroid; *A,* anterior element force; *P,* posterior element force. The line of gravity, trunk center of mass (◇), femoral head (○), and acetabulum (x) landmarks are illustrated, and postural loads acting on the IVDs are shown as shades of gray. Other parameters are defined in the text.

segment was obtained by multiplying the VB modulus by the ratio of the VB cross-sectional area divided by the respective VB height at the centroid. For this analysis, the VB modulus was assumed to be 25 MPa for all segments.[21,22]

The deformed anterior and posterior vertebral body geometry (h_A and h_P) of each VB segment was computed as $h_P - d_P$ and $h_A - d_A$. For the kyphosis deformity analysis that follows, it was assumed that there were no changes in disc geometry, and that the discs did not undergo age-dependent disc degeneration. The model is capable of simulating senile kyphosis (disc degeneration), but the results presented in this report are restricted to osteoporotic kyphosis.

After the anterior and posterior vertebral body deformation had been determined, a coordinate transformation was applied to each vertebral quadrilateral to restore the original discgeometry. The transformation involved rotation of the VB quadrilateral about the VB centroid to restore the original, unloaded VB angleα. Beginning at the L5 segment, the VB quadrilateral was translated in the x and y axes such that the distance from the L5 posteroinferior node to the S1 posterosuperior node (posterior disc height) was restored to the undeformed posterior disc height along a line projected caudally from the posterior nodes of the S1 segment. This process was repeated with each successively more superior segment. The anterior shift in the LOG associated with the progression of the kyphotic deformity was calculated as the mean shift in the C2–S1 VB centroid.

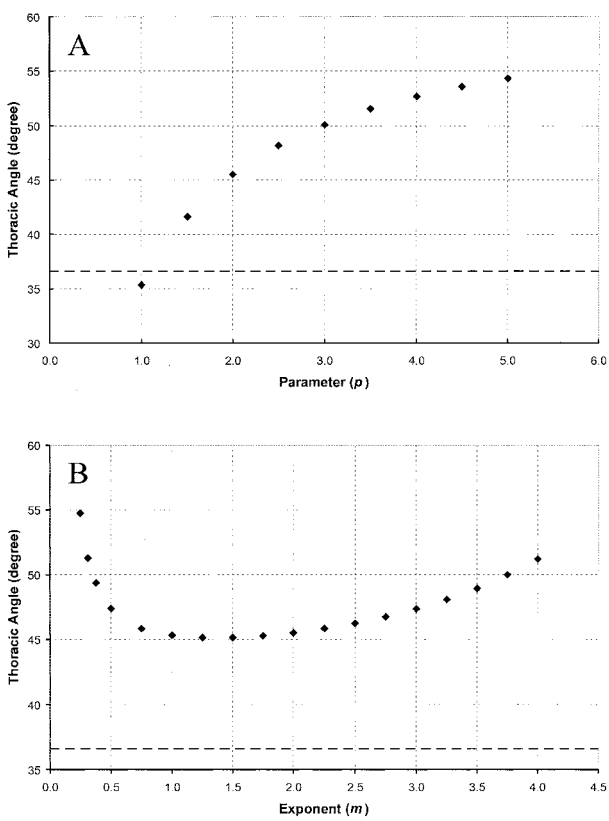

Figure 3. Variation in thoracic angle with the scaling parameter *p* (**A**) and stiffness reduction exponent *m* (**B**). Results shown are for the 1000-N ultimate compressive force model. The dashed line corresponds to the initial neutral posture thoracic angle.

Stiffness Reduction Algorithm. In both the normal and osteopenic vertebral bodies, the stress intensity (tissue stress/apparent stress) or stress concentrations in trabecular bone are up to 100 times greater than the applied or apparent stress.[25,27,35,36] To mimic the local stress concentrations acting on the vertebral body trabecular bone, the VB stiffness was decreased using a stiffness reduction equation (equation 3) derived from a nonlinear load-deformation relation based on plasticity theory[4]:

$$k_d = F_{uLT} * \tanh((k_0 * x/F_{uLT})^m)^{1/m} * (1 - \tanh((k_0 * x/F_{uLT})^m)^2) * (k_0 * x/F_{uLT})^m / x / \tanh((k_0 * x/F_{uLT})^m) \quad (3)$$

where k_d is the reduced or damaged stiffness (N/mm), F_0 is the ultimate compressive strength (N), x is the deformation of the

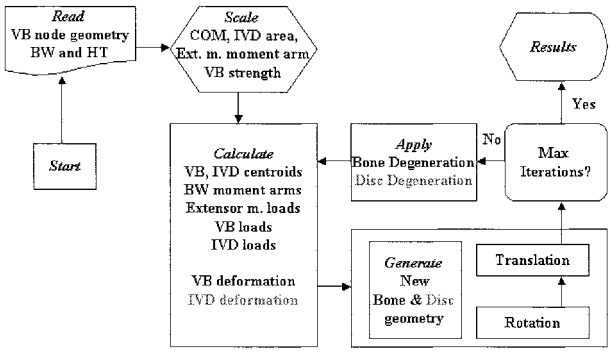

Figure 4. Schematic illustration of the kyphosis model simulation process. Note that the model can accommodate changes in intervertebral disc (IVD) geometry and degeneration, but such changes are not considered in this study.

VB centroid, k_0 is the initial undamaged stiffness (N/mm), and m is an empirical exponent. Equation 3 indicates that the segment stiffness decreases in a nonlinear (hyperbolic) manner with increasing deformation, which is consistent with the nonlinear stress–strain behavior of vertebral trabecular bone observed experimentally.[17] The exponent m in equation 3 influences the amount of deformation required for stiffness reduction or damage initiation. A parametric analysis was performed to determine the influence of the exponent m on the thoracic deformity (Figure 3B). Realistic values for m range from 2 to 4 for bone.[25] In this study, m was assumed to equal 2. After k_d had been determined for each VB quadrilateral, a second loading iteration was performed. The geometry normalization and stiffness reduction process is schematically illustrated in Figure 4.

Changes in the VB strength or degeneration associated with aging in terms of years then were simulated by varying the L3 vertebral compressive force at failure (F_{ult}, N) according to experimental data published by Hansson[13]:

$$F_{ult} = -75\text{Age} + 8199 \qquad (4)$$

This linear relation indicates that by the age of 90 years, the force required to produce failure of the L3 lumbar vertebrae is 1449 N, or approximately one fourth of the compressive failure force at the age of 30 years (equation 4, F_{ult} = 5949 N). The ultimate compressive strength (F_{uLT}) of each VB segment was adjusted (normalized) to the L3 F_{uLT} value times the ratio of the segment disc area divided by the L3 disc area squared. Likewise, the VB stiffness values (k_0) were obtained by multiplying the L3 elastic modulus (25 N/m^2)[21,22] by the VB cross-sectional area/VB height. In this study, forces representative of elderly subjects (equation 4, >80 years, F_{ult} < 2250 N) were simulated and compared with a baseline model approximating a 30-year-old subject (equation 4, F_{ult} ~ 6000 N). The analytical results for variations in the L3 compressive force at failure ranging from 750 to 2250 N in 50-N increments were examined.

Compressive stresses were computed for each of the IVD and VB centroids. For these calculations, the VB midheight cross-sectional area was approximated as 90% of the adjacent (superior) IVD cross-sectional area.

■ Results

The analytical model reproduces the salient features of spinal deformities caused by osteoporotic wedge fractures, namely, increased thoracic kyphosis (Figure 5). Changes in the thoracic angle and the concomitant spinal height change were most apparent when the L3 ultimate compressive force was less than 1500 N. The most osteopenic model (L3 F_{ult} = 750 N) produced gross deformities of the spine, including anterior wedge-like fracture deformities at T7 and T8 (~10° kyphotic deformity at T7). The baseline T7–T8 disc force was 628 N. In the baseline model, the mean disc forces were 122 N (range, 107–133 N) for the cervical region, 560 N (range, 162–821 N) for the thoracic region, and and 615 N (range, 588–667 N) for the lumbar region.

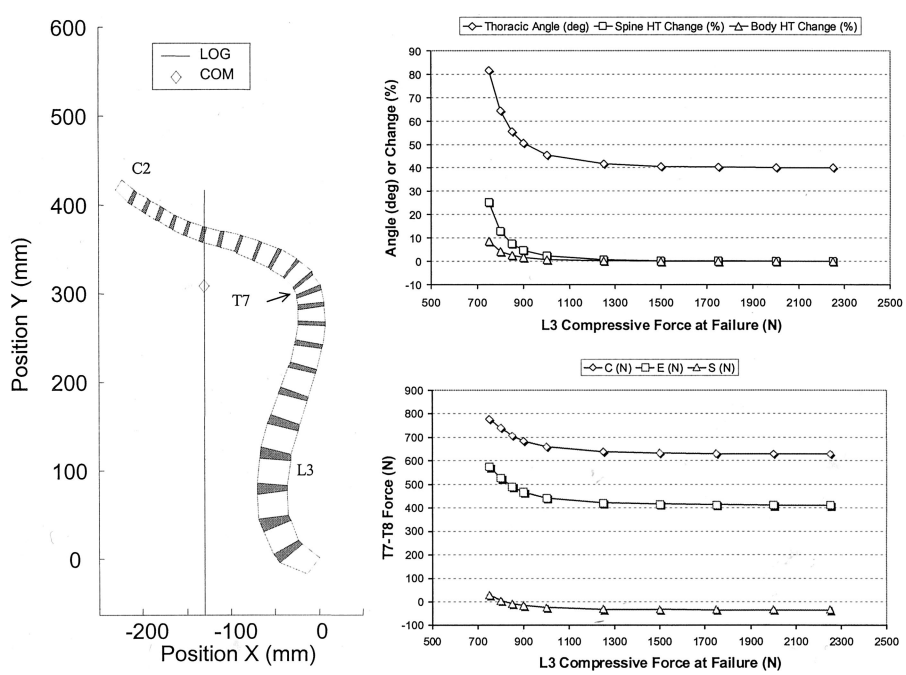

Figure 5. Summary of vertebral deformity simulation results. Left: Graphical depiction of 750-N ultimate compressive force (L3) model. Vertebral body (VB) compression fractures, including T7 and T8 wedge-like deformities, resulted in a 15.1-cm decrease in stature. Upper right: Changes in thoracic angle (°), spine height (%), and body height (%) associated with age-simulated variations in VB ultimate compressive force. Lower right: Changes in T7–T8 intervertebral disc (IVD) forces (*C* and *S*) and extensor muscle force (*E*) associated with age-simulated variations in VB ultimate compressive force.

Table 1. Geometry Characteristics of the Baseline (L3 F_{ult} = 6000 N) and Most Osteopenic (L3 F_{ult} = 750 N) Vertebral Deformity Models

Model F_{ult} (N)	Total Spine HT (mm)	Ant. VB HT (mm)	Post. VB HT (mm)	C2 Shift (mm)	L4 Shift (mm)	Cervical Angle C_2–C_7 (deg)	Thoracic Angle T_2–T_{10} (deg)	Lumbar Angle T_{12}–L_5 (deg)
6000	596.3	497.6	507.1	0	0	−11.2	39.9	−52.6
750	445.8	447.3	479.8	−151	−4.49	−10.3	81.6	−52.3
Δ	150.5	50.3	27.3	−151	−4.49	−0.9	−41.7	−0.3

HT = height; VB = vertebral body; Ant. = anterior; Post. = posterior.

In the most osteopenic model, the increase in thoracic kyphosis (41.7° increase) and the decrease in VB height (7.7% total height reduction) resulted in a 25.2% decrease in spinal height (C2-S1) and an 8.6% decrease in total body height, as compared with the baseline model (Table 1). The resulting deformity produced a 15.1-cm anterior translation of C2 vertebral centroid, which in turn was associated with a 19% increase in compressive force, a 24% increase in compressive stresses, and a 40% increase in paraspinal extensor muscle force at T7–T8. Table 1 summarizes the baseline model geometry predictions, with deformity predictions representative of the osteopenic (L3 F_{ult} = 750 N) subject.

The compressive stresses were greatest in the lower thoracic region, where stresses approached 1.3 MPa in the case of the 750-N ultimate compressive force model (Figure 6a). In the baseline model, the mean disc stresses were 0.50 MPa (range, 0.42–0.61 MPa) for the cervical region, 0.83 MPa (range, 0.47–1.01 MPa) for the thoracic region, and 0.48 MPa (range, 0.45–0.53 MPa) for the lumbar region. Figure 6b compares the IVD compressive and shear loads with the corresponding extensor muscle loads associated with the 1250-N ultimate compressive force model. Peak muscle and IVD compressive loads were located at the T11–T12 segment, whereas the peak IVD shear load was at L1–L2. Thoracolumbar segment loads increased as the thoracic kyphosis angle increased during the aging process (Figure 7).

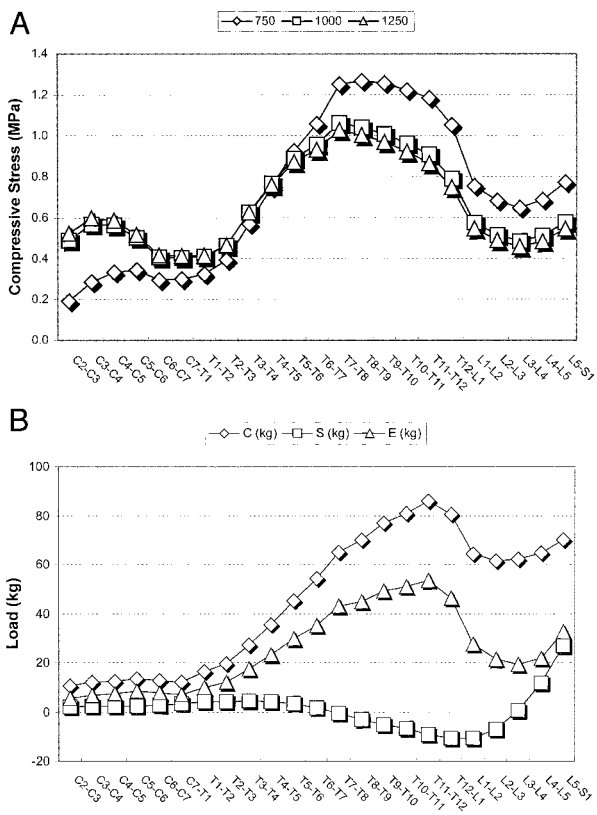

Figure 6. **A,** Intervertebral disc (IVD) compressive stress variations with segment level for the 750-N, 1000-N, and 1250-N ultimate compressive force (L3) models. **B**, Variations in IVD compressive load, IVD shear load, and extensor muscle load with segment level (L3 750-N ultimate compressive force model).

Discussion

The vertebral deformity model presented in this report confirms the authors' hypothesis that osteoporotic thoracic kyphosis deformities in elderly subjects are promoted by postural forces, and are subsequently exacerbated by anterior translation of the head and upper torso. In the presence of osteoporosis, the physiologic kyphosis and increased stresses at the anterior margins of the thoracic vertebral bodies produce prominent wedging of the mid-thoracic vertebrae. Fractures and marked deformities are predicted to occur when the ultimate compressive force of the seventh thoracic vertebrae decreases to 56% of the body force (T7 compressive strength < 421 N, L3 compressive strength < 1250 N). According to the *in vitro* mechanical test and densitometry data of Hansson,[13] the latter corresponds to an L3 vertebral bone mineral content (BMC) of 1.63 g/cm and an apparent age of 93 years. Hansson[13] also noted that

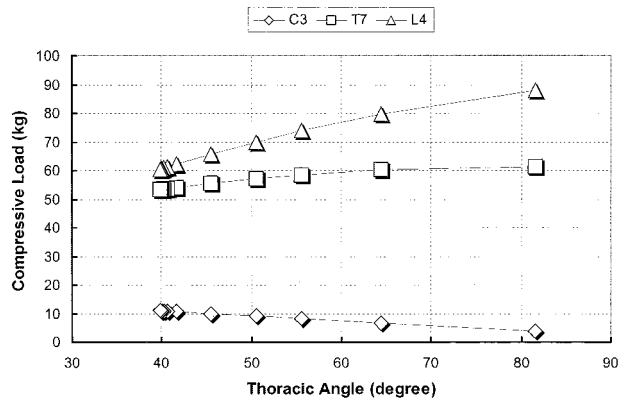

Figure 7. Relation between vertebral compressive load and thoracic angle for the C3, T7, and L4 vertebral segments.

the ultimate compressive force of the human lumbar vertebral centrum is as low as 952 N. As shown in the kyphosis model simulations, when the L3 vertebral strength decreases to this level, failure of the vertebral structures can occur under loads imposed by the weight of the body above the vertebrae. In this study, vertebral deformities were further exacerbated by anterior translation of the upper spinal column, which acts to increase compressive loads in the thoracolumbar region of the spine.

In normal and osteopenic thoracolumbar vertebrae, compression fractures that result from fatigue damage or low force trauma generally are undetectable on conventional radiographs.[15] Vertebral compression fractures occur when the load applied to the vertebral structures exceed their ability to support that load. Four characteristic types of fractures are formed during overloading of the vertebral body: central endplate, Schmorl's node, wedge, and burst. Central endplate fractures often are the first sign of failure observed during *in vitro* compression fatigue loading experiments conducted on normal and osteopenic human lumbar vertebral motion segments.[16] Hansson *et al*[14] also noted that Schmorl's nodes were predominantly associated with segments from younger subjects who had less degenerated discs, whereas central endplate fractures were predominantly associated with older, more degenerated specimens. A combination of central endplate fracture and anterior wedge type fracture are formed during compression–flexion loading of lumbar vertebrae.[10] As the severity of endplate fractures and Schmorl's nodes increases, the characteristic biconcave curvature of the endplates and vertebral body height reduction become evident on radiographs (Figure 1). Indeed, for many clinicians, radiographically detectable compression fractures represent the first verified presence of osteoporosis or bone fragility.

The normal human spinal column is a highly loaded structure. Compressive forces as high as 7000 N are predicted to act on lumbar vertebrae during the performance of maximum-exertion isometric trunk extension tasks.[11] The vertebrae in a young, healthy individual readily tolerate such forces. The kyphosis model, however, demonstrates how remarkably close to failure the elderly human vertebral body is when it comes to continuous stresses associated with body weight loading or exposure to cyclic stresses associated with repetitive loading. Indeed, compressive forces as low as 50% of the single-cycle failure strength of the vertebrae produce fatigue fractures after fewer than 1000 cycles.[16] The predictions of the current model indicate therefore that repetitive loading in an elderly subject with a single-cycle thoracic vertebral compressive strength less than 2500 N (76-year-old subject, equation 4) would result in thoracic wedge fractures and concomitant thoracic kyphosis deformity. Body weight loading in a subject with a thoracic vertebral compressive strength of 1250 N would produce equivalent deformities. Such findings are consistent with reports of compression fracture occurring spontaneously or after trivial strain.[32]

The kyphotic deformity produced by the biomechanical simulation, including the T7 wedge fracture formation and the magnitude of the thoracic kyphosis, closely resembles the deformities seen clinically and illustrated in Figure 1. Deformities such as that illustrated in Figure 1, although not a common occurrence, are prevalent in more elderly female subjects. However, some degree of thoracic kyphosis is common in most postmenopausal women with osteoporosis. In a study of 98 postmenopausal women (mean age, 69 years), Cortet *et al*[5] found an average increase in thoracic kyphosis deformities of 11° for women with radiographic evidence of fracture, as compared with women who had no radiographic evidence of fracture. Assuming that the normal T2–T10 thoracic kyphosis is 40°,[4] this increase corresponds to a 51° angle of kyphosis.[9] In a subject with a body weight of 77 kg and a height of 177 cm, the current analytical model predicts that the L3 lumbar compressive vertebral strength and the L3 vertebral stiffness corresponding to such a thoracic deformity would be 900 N and 960 N/mm, respectively. For such an individual, the corresponding thoracic (T7) compressive strength would be 421 N, and the stiffness would be 99 N/mm.

Regarding the predictions of the current model, it is important to note that several assumptions were made to obtain estimates of the strength and stiffness of the vertebrae. First, the empirical data of Hansson[13] were used to establish the compressive strength of the L3 vertebrae. Because compressive strength is a structural property, a higher compressive strength would be predicted for larger subjects and *vice versa*. Moreover, in this study it was assumed that the compressive strength and the stiffness of the other vertebrae in the model could be scaled using the vertebral height, disc height, and disc cross-sectional area of the vertebral segments. Thus, segments in different regions of the spine and segments from subjects with larger vertebrae would be predicted to have a corresponding higher compressive strength and stiffness, and *vice versa*. This is a reasonable assumption provided the material or mechanical properties of the C2–S1 spine segments are equivalent. Previous experimental studies, however, indicated that the mechanical properties of human lumbar vertebrae are closely dependent on the degree of disc degeneration.[13,24] Recognizing that the degree of disc degeneration can vary substantially for different levels of the spine,[41,42] it is apparent that certain levels of the spine may undergo nonuniform degradation in their stiffness and compressive strength properties. In this study, it was assumed that the spine undergoes uniform degradation in strength, and no influences of disc degeneration or other pathologic conditions were considered, including congenital anomalies or posttraumatic lesions.

Another limitation of the current study was the lack of direct experimental validation for the model predictions. Because this report focuses on age-dependent and progressive strength changes in the C2–S1 human spine, experimental validations are difficult, if not impossible, to perform. In addition, the deformity model incorporates

two mathematical parameters (m and p) that influence the rate of kyphotic deformity progression. Both of these parameters influence the rate of deformity progression, and in this report, conservative values were chosen for the simulations. It was noted, however, that the thoracic deformity (81.6° kyphosis angle associated with the most osteopenic ultimate compressive force model) corresponded very closely to the clinical presentation of osteoporotic kyphosis deformities (Figure 1).[6,20,37]

The compressive forces and stresses determined by the model also agree with previous numerical simulations[18,39] and experimental results based on intradiscal pressure measurements.[1,34,38] In a recent study, Sato *et al*[34] measured L4–L5 intradiscal pressures and calculated L4–L5 disc loads for several upright postures in eight healthy volunteers (ages, 22–29 years; weight, 73 kg; height, 173 cm) and 28 patients (ages, 19–74 years; weight, 68 kg; height, 165 cm) with low back pain. In the normal subject group, they reported that the mean upright-posture L3–L4 intradiscal pressure was 0.539 MPa (range, 0.215–0.747 MPa). Taking into account the prone-lying intradiscal pressure (mean, 0.091 Mpa; range, 0.065–0.149 MPa), their results (upright posture minus prone lying) are very consistent with the lumbar region disc compressive stresses reported in the current study. Hence, these and other reported intradiscal pressure measurements corroborate the biomechanical predictions for the lumbar region of the spine, but a rigorous validation of the model deformity and thoracic region load predictions is currently not possible.

The vertebral deformity model presented in this report provides a basic understanding of the apparent forces and stresses acting on the vertebral structures, but does not tell anything about the magnitude of the stresses and strains acting on the trabecular bone tissues that compose the bulk of the vertebral bodies. More explicit mechanical stress–strain behavior and damage prediction in vertebral bone structures can be obtained using numeric techniques such as the finite-element analysis (FEA) method.[8,25,30,36,40] Recent structural FEA studies of human vertebrae[35,36] indicate that the stress intensity or stress concentrations in trabecular bone are up to 100 times greater than the applied or apparent stress (force/surface area). Hence, osteopenic bone may be damaged at relatively low loads, such as thoracic load magnitudes associated with upright-posture weightbearing. Indeed, findings have shown that thoracic hyperkyphosis in osteoporotic subjects is related to anterior compression fractures.[6,20] In the current study, the authors mimicked the effects of stress concentrations in trabecular bone by using a vertebral stiffness reduction algorithm based on plasticity theory.[4,5] Finite-element analysis of anatomically accurate osteopenic thoracic vertebrae indicate that the nonlinear compressive stress–strain behavior and modulus reduction (bone damage) of thoracic vertebrae are well represented using plasticity theory.[25,27]

In conclusion, the analytical model presented in this report reproduces the general characteristics of spinal deformities caused by osteoporotic wedge fractures. These results suggest that exercises, bracing or other rehabilitative procedures aimed at reducing the anterior translation of the cervicothoracic spine and thoracic hyperkyphosis, may be beneficial in reducing the risk or occurrence of osteoporotic fractures. Future applications of the model include simulations of minimally invasive surgical procedures, such as percutaneous transpedicular vertebroplasty. In vertebroplasty, polymethylmethacrylate bone cement is used to augment the strength and stiffness of vertebral bodies,[2,3] and is purported to preserve spinal alignment and to decrease chronic pain in patients with vertebral compression fractures and thoracic kyphosis.[7,26] The increased vertebral segment strength and stiffness provided by vertebroplasty can be studied using the C2–S1 spine deformity model. Additional model development work also is needed to study the combined effects of vertebral body height reduction (osteoporotic kyphosis) and intervertebral disc height reduction (senile kyphosis), as well as the effects of forces associated with mechanical overload caused by activities such as lifting and exercise.

■ Key Points

- A biomechanical model has been developed to predict the progression of osteoporotic thoracic kyphosis.
- Compressive stresses associated with postural forces were greatest in the midthoracic region of the spine.
- Changes in the thoracic angle and the concomitant spinal height change were most marked when the T7 vertebral body compressive strength decreased to less than 1500 N.
- Model data may provide insight for surgical and rehabilitative procedures used to treat thoracic hyperkyphosis.

Acknowledgments

The authors thank the following funding agencies for their support of this research: Vermont Space Grant Consortium, NASA EPSCoR, Chiropractic Biophysics NonProfit, and the Foundation for the Advancement of Chiropractic Education.

References

1. Adams MA, Hutton WC. The effect of posture on the lumbar spine. J Bone Joint Surg [Br] 1985;67:625–9.
2. Belkoff SM, Mathis JM, Erbe EM, et al. Biomechanical evaluation of a new bone cement for use in vertebroplasty. Spine 2000;25:1061–4.
3. Belkoff SM, Mathis JM, Jasper LE, et al. The biomechanics of vertebroplasty: The effect of cement volume on mechanical behavior. Spine 2001;26:1537–41.
4. Betten J. Generalization of nonlinear material laws found in experiments to multiaxial states of stress. Eur J Mech-A/Solids 1989;8:325–39.
5. Cortet B, Houvenagel E, Puisieux F, et al. Spinal curvatures and quality of life in women with vertebral fractures secondary to osteoporosis. Spine 1999; 24:1921–5.
6. De Smet AA, Robinson RG, Johnson BE, et al. Spinal compression fractures in osteoporotic women: Patterns and relationship to hyperkyphosis. Radiology 1988;166:497–500.

7. Garfin SR, Yuan HA, Reiley MA. New technologies in spine: Kyphoplasty and vertebroplasty for the treatment of painful osteoporotic compression fractures. Spine 2001;26:1511–5.
8. Gilbertson LG, Goel VK, Kong WZ, et al. Finite-element methods in spine biomechanics research. Crit Rev Biomed Eng 1995;23:411–73.
9. Goh S, Price RI, Leedman PJ, et al. Age-independent correlation of optically determined thoracic kyphosis with lumbar spine bone mineral density. J Musculoskel Res 1999;3:267–74.
10. Granhed H, Jonson R, Hansson T. Mineral content and strength of lumbar vertebrae: A cadaver study. Acta Orthop Scand 1989;60:105–9.
11. Guzik DC, Keller TS, Szpalski M, et al. A biomechanical model of the lumbar spine during upright isometric flexion, extension, and lateral bending. Spine 1996;21:427–33.
12. Hall SE, Criddle RA, Comito TL, et al. A case–control study of quality of life and functional impairment in women with long-standing vertebral osteoporotic fracture. Osteoporos Int 1999;9:508–15.
13. Hansson T. The bone mineral content and biomechanical properties of lumbar vertebrae. PhD thesis. University of Göteborg, Göteborg, Sweden, 1977.
14. Hansson T, Keller T, Jonson R. Fatigue fracture morphology in human lumbar motion segments. J Spinal Disord 1988;1:33–8.
15. Hansson T, Keller TS. Osteoporosis of the spine. In: Wiesel SW, Weinstein JN, Herkowitz H, et al, eds. The Lumbar Spine. 2nd ed. Philadelphia: WB Saunders, 1996:969–88.
16. Hansson TH, Keller TS, Panjabi MM. A study of the compressive properties of lumbar vertebral trabeculae: Effects of tissue characteristics. Spine 1987; 12:56–62.
17. Harrison DE, Cailliet R, Harrison DD, et al. How do anterior/posterior translations of the thoracic cage affect the sagittal lumbar spine, pelvic tilt, and thoracic kyphosis? Eur Spine J 2002;11:287–93.
18. Harrison DE, Harrison DD, Janik TJ, et al. Comparison of axial and flexural stresses in lordosis and three buckled configurations of the cervical spine. Clin Biomech 2001;16:276–84.
19. Harrison DE, Janik TJ, Harrison DD, et al. Can the thoracic kyphosis be modeled with a simple geometric shape? The results of circular and elliptical modeling in 80 asymptomatic patients. J Spinal Disord Tech 2002;15:213–20.
20. Johansson C, Mellstrom D, Rosengren K, et al. Prevalence of vertebral fractures in 85-year-olds: Radiographic examination of 462 subjects. Acta Orthop Scand 1993;64:25–7.
21. Keller TS. Predicting the compressive mechanical behavior of bone. J Biomech 1994;27:1159–68.
22. Keller TS, Hansson TH, Abram AC, et al. Regional variations in the compressive properties of lumbar vertebral trabeculae: Effects of disc degeneration. Spine 1989;14:1012–9.
23. Keller TS, Nathan M. Height change caused by creep in intervertebral discs: A sagittal plane model. J Spinal Disord 1999;12:313–24.
24. Keller TS, Ziv I, Moeljanto E, et al. Interdependence of lumbar disc and subdiscal bone properties: A report of the normal and degenerated spine. J Spinal Disord 1993;6:106–13.
25. Kosmopoulos V, Keller TS, Liebschner MA. Finite element modeling of vertebral damage and repair. *10th Annual Symposium on Computational Methods in Orthopaedic Biomechanics*, UT Southwestern Medical Center, Dallas, TX, Session 2:Spine. February 9, 2002.
26. Lieberman IH, Dudeney S, Reinhardt MK, et al. Initial outcome and efficacy of "kyphoplasty" in the treatment of painful osteoporotic vertebral compression fractures. Spine 2001;26:1631–8.
27. Liebschner MA, Rosenberg WS, Keaveny TM. Effects of bone cement volume and distribution on vertebral stiffness after vertebroplasty. Spine 2001; 26:1547–54.
28. Lyles KW, Gold DT, Shipp KM, et al. Association of osteoporotic vertebral compression fractures with impaired functional status. Am J Med 1993;94: 595–601.
29. Melton LJ III, Lane AW, Cooper C, et al. Prevalence and incidence of vertebral deformities. Osteoporos Int 1993;3:113–9.
30. Mizrahi J, Silva MJ, Keaveny TM, et al. Finite-element stress analysis of the normal and osteoporotic lumbar vertebral body. Spine 1993;18:2088–96.
31. Osteoporosis Prevention, Diagnosis, Therapy. NIH Consensus Statement 2000;17:1–36.
32. Patel U, Skingle S, Campbell GA, et al. Clinical profile of acute vertebral compression fractures in osteoporosis. Br J Rheumatol 1991;30:418–21.
33. Ruff S. Brief acceleration: Less than one second. Ger Aviat Med World War II 1950;1:584–97.
34. Sato K, Kikuchi S, Yonezawa T. *In vivo* intradiscal pressure measurement in healthy individuals and in patients with ongoing back problems. Spine 1999; 24:2468–74.
35. Saxena R, Keller TS. A volumetric finite-element scheme to investigate the mechanical properties of normal and osteoporotic trabecular bone. In: Pedersen P, Bensøe MP, eds. Dordrecht: Kluwer Academic, 1999:373–86.
36. Saxena R, Keller TS, Sullivan JM. A three-dimensional finite-element scheme to investigate the apparent mechanical properties of trabecular bone. Comput Methods Biomech Biomed Eng 1999;2:285–94.
37. Schmorl G, Junghanns H. The Human Spine in Health and Disease. New York: Grune & Stratton, 1957.
38. Schultz AB, Andersson GB. Analysis of loads on the lumbar spine. Spine 1981;6:76–82.
39. Schultz AB, Andersson GB, Haderspeck K, et al. Analysis and measurement of lumbar trunk loads in tasks involving bends and twists. J Biomech 1982; 15:669–75.
40. Suwito W, Keller TS, Basu PK, et al. Geometric and material property study of the human lumbar spine using the finite-element method. J Spinal Disord 1992;5:50–9.
41. Videman T, Battie MC, Gill K, et al. Magnetic resonance imaging findings and their relationships in the thoracic and lumbar spine: Insights into the etiopathogenesis of spinal degeneration. Spine 1995;20:928–35.
42. Yoshimura N, Dennison E, Wilman C, et al. Epidemiology of chronic disc degeneration and osteoarthritis of the lumbar spine in Brain and Japan: A comparative study. J Rheumatol 2000;27:429–33.